

## CHAPTER IV

### EXTREMELY HIGH SURFACE AREA OF ORDERED MESOPOROUS MCM-41 BY ATRENE ROUTE

#### 4.1 Abstract

Silatrane synthesized from inexpensive oxide precursor, silica and TEA was used as the precursor for MCM-41 synthesis at low temperature because of its stability in aqueous solutions. Using cationic surfactant hexadecyltrimethyl ammonium bromide (CTAB) as a template, the resulting meso-structure mimics the liquid crystal phase. Varying the surfactant concentration, ion concentration and temperature of the system, changes the structure of the liquid crystal phase, resulting in different pore structures and surface area. After heat treatment, very high surface area mesoporous silica was obtained and characterized by using XRD, BET and TEM. XRD and TEM results show a clear picture of hexagonal structure. The surface area is extraordinarily high, up to more than 2400 m<sup>2</sup>/g with pore volume of 1.29 cc/g. However, the pore volume is up to 1.72 cc/g when the surface area is greater than 2100 m<sup>2</sup>/g.

#### 4.2 Introduction

The application of oligomers and polymers as templates in the synthesis of mesoporous silica and other mesoporous oxides has recently attracted much attention and led to the development of convenient synthetic pathways for materials with tailored porous structures and desirable morphologies. Many different types of oligomeric and polymeric templates have already been employed in the synthesis of mesoporous oxides. It was demonstrated that oligomers, such as alkyl poly(ethylene oxide) and alkylphenyl poly(ethylene oxide) surfactants, are facile supramolecular templates [1-3]. The use of liquid crystal phase of oligomeric surfactant under acidic conditions is employed for the preparation of hexagonal and cubic mesoporous silica

[4]. The synthesis in neutral media afforded disordered mesoporous silica with large specific surface area and quite uniform pores.

Metal alkoxides are very useful precursors for producing mesostructured materials. Atrane precursors provide a very versatile route to obtain ordered mesoporous material. Normally, the syntheses of atrane complexes were carried out by means of transesterification reaction, starting from alkoxy derivatives in non-aqueous dried solvents under an inert atmosphere. Haskouri et al. studied mesoporous material synthesis, having a solution containing the metal atrane precursor mixed with a surfactant in alkaline aqueous solution [5-7]. The procedure is quite complicated. Moreover, the alkoxide precursor used for the atrane complex synthesis is commercially expensive [8-9]. Wongkasemjit et al. [10-11] synthesized the silatrane precursor directly from inexpensive metal oxide,  $\text{SiO}_2$ , and triethanolamine via the "Oxide One Pot Synthesis (OOPS)" process, giving very high purity of silatrane product. The synthesized silatrane from the OOPS process has been successfully used for synthesis of high quality microporous zeolite, such as LTA [12], ANA, GIS [13] and MFI [14]. In this manuscript we report the results of our studies of a new synthetic route to remarkably high surface area MCM-41 using silatrane as the precursor and hexadecyltrimethyl ammonium bromide (CTAB) as a template, including investigation of the influence of variables and reaction conditions.

### **4.3 Experimental**

#### **4.3.1 Materials**

Fumed silica ( $\text{SiO}_2$ ) was purchased from Aldrich Chemical Co. Ethylene glycol ( $\text{HOCH}_2\text{CH}_2\text{OH}$ ) and triethanolamine (TEA,  $\text{N}(\text{CH}_2\text{CH}_2\text{OH})_3$ ) were supplied by Labscan and used as received. Acetonitrile ( $\text{CH}_3\text{CN}$ ) was obtained from Labscan and distilled before use. Hexadecyltrimethyl ammonium bromide (CTAB) and sodium hydroxide were purchased from Sigma Chemical Co.

#### **4.3.2 Material Characterization**

Mass spectra of silatrane precursor were obtained using a FISIONS Instruments 707 VG Autospec-ultima mass spectrometer (Manchester, England) with VG data system, using the positive fast atom bombardment (FAB<sup>+</sup>-MS) mode. FTIR spectroscopic analysis was conducted using a Bruker Instrument (EQUINOX55) with a resolution of 4 cm<sup>-1</sup>. Thermal properties were analyzed by thermogravimetric analysis (TGA) using Du Pont Instrument TGA 2950.

The mesoporous product was characterized using a Rigaku X-ray diffractometer at a scanning speed of 2 degree/sec using CuK $\alpha$  as source. The working range was  $2\theta = 1.5-10$ . Electron microscope study (TEM micrographs and electron diffraction patterns) was carried out using JEOL 2010F. Surface area and average pore size were estimated by BET method using a Quantasorb JR. (Autosorb-1). The product was degassed at 250°C for 12 hr/prior to analysis. The calcination was achieved using a Carbolite Furnace (CFS 1200). The heating rate was 5°C/min.

#### 4.3.3 Silatrane Synthesis [Si(TEA)<sub>2</sub>]

Wongkasemjit's synthetic method [10-11] was followed by mixing silicon dioxide, 0.10 mol, and triethanolamine, 0.125 mol, in a simple distillation set using 100 mL ethylene glycol solvent. The reaction was done at the boiling point of ethylene glycol under nitrogen atmosphere to remove water as a by-product along with ethylene glycol from the system. The reaction was run for 10 hr and the rest of ethylene glycol was removed under vacuum (1.6 Pa) at 110°C. The brownish white solid was washed with dried acetonitrile for three times. The white powder product was characterized using FTIR, TGA, DSC and FAB<sup>+</sup>-MS.

FTIR bands, see Fig.4.1 observed were 3000-3700 cm<sup>-1</sup> (w, intermolecular hydrogen bonding), 2860-2986 cm<sup>-1</sup> (s,  $\nu$ C-H), 1244-1275 cm<sup>-1</sup> (m,  $\nu$ C-N), 1170-1117 (bs,  $\nu$ Si-O), 1093 (s,  $\nu$ Si-O-C), 1073 (s,  $\nu$ C-O), 1049 (s,  $\nu$ Si-O), 1021 (s,  $\nu$ C-O), 785 and 729 (s,  $\nu$ Si-O-C) and 579 cm<sup>-1</sup> (w, Si $\leftarrow$ ---N). TGA showed one sharp mass loss transition at 390°C and gave 18.47% ceramic yield corresponding to Si((OCH<sub>2</sub>CH<sub>2</sub>)<sub>3</sub>N)<sub>2</sub>H<sub>2</sub>. FAB<sup>+</sup>-MS showed the highest m/e at 669 of Si<sub>3</sub>((OCH<sub>2</sub>CH<sub>2</sub>)<sub>3</sub>N)<sub>4</sub>H<sup>+</sup> and 100% intensity at 323 of Si((OCH<sub>2</sub>CH<sub>2</sub>)<sub>3</sub>N)<sub>2</sub>H<sup>+</sup>.

#### 4.3.4 Synthesis of MCM-41

0.004 M silatrane precursor was added to a solution containing x mol of CTAB, y mol of NaOH and 0.014 mol of TEA. 0.36 M of water was then added with vigorous stirring. The mixture was stirred for various times to follow the reaction using XRD, BET and TEM. The obtained crude product was filtered and washed with water to obtain a white solid. The white solid was dried at room temperature and calcined at 550°C for 7 hrs to obtain mesoporous MCM-41. In this study, surfactant concentration, ion concentration, mixing temperature and aging time were varied to find an optimum condition.

### 4.4 Results and Discussion

#### 4.4.1 MCM-41 Synthesis

Silica MCM-41 is a member of M41S family with a hexagonal array of two-dimensional pores. Using hexadecyltrimethyl ammonium bromide (CTAB) as a template for the synthesis of mesoporous MCM-41 silica via the liquid crystal templating mechanism (LCT), the pores will mimic the surfactant liquid crystal structure [1-4, 15]. Conventional procedure to synthesize this type of material using SiO<sub>2</sub> as precursor needs to use high temperature and long reaction time in autoclave [16, 19-21, 29]. An alternative way using alkoxide precursor, such as TEOS or TMOS, can reduce reaction temperature and time [15, 24, 30]. Haskouri synthesized MCM-41 from silatrane precursor [5-7] prepared by a more expensive and complicated method [8-9]. In comparison with our method, silatrane is obtained by reacting inexpensive SiO<sub>2</sub> with triethanolamine in a one step synthesis [10-11]. Additionally, our MCM-41 product not only was obtained at lower and shorter reaction temperature and time, respectively, but also impressively shows much higher surface area and pore volume.

#### 4.4.2 Effect of Ion Concentration

Ion concentration is one of the important parameters in micelle formation. Changing ion concentration will affect the size and the structure of liquid crystal. To demonstrate whether using silatrane as alkoxide precursor has advantages in the MCM-41 synthesis, the following formulation of Si: 0.3 CTAB: y NaOH: 3.5 TEA: 90 H<sub>2</sub>O at ambient temperature was used [8-9]; where y was varied in the range of 0.15-1.0. As shown in Fig.4.2, XRD spectra give only hk0 reflections and no reflections at diffraction angles larger than 6 degree 2 $\theta$  was observed. The positions of these peaks approximately fit the position for the hk0 reflections from a hexagonal unit cell with  $a = b$  and  $c = \infty$  [16-17]. Too high NaOH ratios, viz. 1 and 0.5, do not show MCM-41 pattern while the ratios of 0.25 and 0.35 clearly show a pattern of MCM-41 at 3 peak positions of 100, 110 and 200 reflections of long range structural ordering. The results showed the effect of ion to liquid crystal formation. Normally, addition of electrolyte causes a decrease in electrical repulsion between ionic heads due to shielding by counter ions, thus resulting in a decrease in CMC of CTAB [18]. However, at high ionic concentrations charge repulsion occurs, inhibiting the hexagonal array to form. By comparing between the ratios of 0.25 and 0.35, from BET results, the surface area of the 0.25 NaOH ratio is higher and the pore size is smaller than the 0.35 NaOH ratio, as shown in table 4.1. That means, the liquid crystal in the solution containing 0.25 NaOH ratio is more compact than that in the 0.35 NaOH solution.

#### 4.4.3 Effect of Temperature

It is known that temperature also affects to the liquid crystal formation, thus the temperature effect was investigated. The ratio of 0.25 NaOH was chosen due to the higher surface area obtained. When increasing the mixing temperature from 40°C to 100°C at the formulation of Si:0.3CTAB:0.25NaOH:3.5TEA:90H<sub>2</sub>O, the XRD spectra showed the sharper peaks and slightly shifted peaks to the lower degree two theta (Fig.4.3), indicative of larger pores and more better alignment. The reason is that the higher temperature makes the surfactant tails move or vibrate more flexibly or freely, resulting in a larger molecular volume for the surfactant molecules,

consequently leaving behind a larger pore after removal [19-22]. Zhou *et al* [19] reported that the mechanism of channel growth relies on the interaction between the silicate anion and the surfactant molecule. His study using HRTEM showed that the process was diffusion controlled. At high temperatures the entire process quickly resulted in uniform channel diameter and gave maximum diameter of the surfactant rod [19]. In our case too increasing the temperature up to 60°C resulted in XRD spectra showing clearer pattern of MCM-41, and clearer separation of the 110 and 200 reflections caused from long range ordering of hexagonal array.

To confirm the XRD results, TEM image of MCM-41 at 60°C was analyzed and is shown in Fig 4.4. Fig 4.4a shows a hexagonal arrangement corresponding to the straight channels of MCM-41 along the channel direction or the incident beam is along the 001 direction. Fig. 4.4b is the TEM image in the perpendicular direction, cylindrical cross sections of the channels are clearly visible. Normally, the pore diameter is calculated from the perpendicular direction because the image projected along the incident beam may give somewhat less than actual value [17].

TEM results shown in Fig. 4.5 give larger pore sizes when increasing temperature which is in agreement with the results of XRD spectra. The diameters of the channel calculated from Fig.4.5a and 4.5b are 23.5 Å and 31.3 Å, respectively. Furthermore, channel diameter from sorption measurements using Barrett-Joyner-Helenda (BJH) formula provides the same results as XRD and TEM. The average pore diameters of MCM-41 at higher temperatures are also larger than those at lower temperatures. The diameters at 60° and 100°C are 22 Å and 35 Å, respectively, which is close to the size of CTABr micelle, 39.7 Å. Cheng *et al*'s study demonstrated that the channel diameter of MCM-41 obtained from the reaction time of 48 hrs using sorption technique increased from 27.1 Å to 36.5 Å when increasing temperature from 70° to 165°C [20]. In our case, the reaction time is only 3 hrs and the diameter at 100°C is comparable to his at 165°C. In addition, it was reported that pore size and uniformity of product prepared under identical conditions but different silicate anions are varied due to the different diffusion rate of silicate anions from different sources of silica [21]. Our precursor, silatrane, is an easily formed silicate anion under basic conditions so it may diffuse and undergo condensation faster while

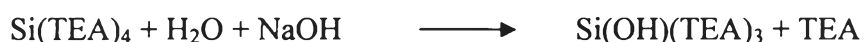
maintaining the pore structure. In fact, to synthesize larger pore MCM-41 materials long chain surfactants [12, 23-24] and a swelling agent [21, 25-26] are needed. However, they are not easy to obtain and thus are very expensive. Moreover, the swelling agent expands the pore size product, but decreases the quality of the product.

Surface areas and pore volumes of MCM-41 obtained from our silatrane are very high and much higher than atranes synthesized by another route [5-7], as shown in table 4.2. As can be seen, the BET surface area decreased while the pore volume increased with increasing reaction temperature. However, at 100°C the reversed trend was observed. The reason may come from some collapse of pore structure when increased reaction temperature. The highest surface area in Haskouri *et. al.*'s work using silatrane prepared by other routes [8-9] is approximately twice lower than ours. The reason probably comes from higher purity and more homogeneity of silatrane precursor prepared using Wongkasemjit's synthetic method [10-11], as indicated by only one sharp mass loss transition of TGA and high intensity of XRD spectrum.

#### 4.4.4 Effect of Aging Time

In this study, since alkoxide precursor is used to prepare MCM-41 via sol-gel process, involving hydrolysis and condensation reactions, aging time, representing the time between the formation of gel and the removal of solvent, is also one of the important factors. For alkoxide derived gel, condensation between functional groups on the surface continues to occur after gel point. During aging, there are changes in most texture and physical properties of the gel [27-28]. The strength of the gel thereby increases with aging. In this case, hydrolysis and condensation of silatrane gave Si-O-Si linkage, as shown below.

##### Hydrolysis:



##### Condensation:



Although the MCM-41 synthesis was claimed to depend only on the type of silicate and surfactant used [29] it is interesting to prove whether aging time indeed

affects the MCM-41 formation. By fixing the formula of Si:0.3CTAB:0.25NaOH:3.5TEA:90H<sub>2</sub>O and the mixing temperature at 60°C, aging time was varied from 1 to 12 hr. The XRD results of all aging time are shown in fig. 4.6. For 1 and 2 hr aging time, it showed broader band and lower intensity comparing with the others. However, increasing aging time up to 3 hr, it showed no significance from the aging factor. The reason could possibly drawn that silicate ion needs time to diffuse and aggregate around rod shape micelle, causing condensation reaction to occur. Thus, at too short aging time, the condensation may not be complete to form high quality MCM-41. However, it shows that the reaction time used in this case is much shorter than other reported studies. BET surface areas, pore sizes and pore volumes summarized in Table 4.3 show no differences either.

#### 4.4.5 Effect of Surfactant Concentration

The formula of Si:yCTAB:0.25NaOH:3.5TEA:90H<sub>2</sub>O where y is in the range of 0.2 to 0.6, was used to test the effect of surfactant concentration on the quality of MCM-41 formed at the mixing temperature of 60°C. Fig.4.7, shows the XRD spectra as a function of the surfactant ratio. At the lowest surfactant ratio of 0.2, XRD peaks are somewhat broader when compared with the others. This result is in agreement with Cheng's work. He proposed a mechanism for surfactant micelle catalyst, which relies on electrostatic interaction at the micelle-silicate interface. The Br<sup>-</sup> and OH<sup>-</sup> ion exchange in the surfactant accelerates the hydrolysis and condensation of organosilicate. The increasing exchange rate will increase the basicity of the micelle surface, promoting hydrolysis and condensation [30]. Thus, low surfactant ratios may not be enough to give high quality MCM-41. The BET surface area results in Table 4.4 show an increase in surface area with increasing surfactant ratio, but there is no difference in pore size, meaning that the micelle size is not affected by the increasing the surfactant concentration. The highest surface area obtained is as high as 2430 m<sup>2</sup>/g. At the reaction temperature of 100°C, the surface areas decreased while the pore volume significantly increased. This is due to the thermal expansion of micelle, as discussed earlier, which increases the volume of liquid crystal. At the surfactant ratio of 0.6, the surface area and the pore volume are



as high as 2100 m<sup>2</sup>/g and 1.723 cc/g, respectively. The average pore sizes are larger, as predicted.

The TEM images of MCM-41 obtained using the 0.6 surfactant ratio are shown in Fig.4.3. Hexagonal arraying of the pores can be clearly seen. In addition, increasing the mixing temperature from 60° to 100°C also showed the same trend as shown in Fig.4.3. The XRD peak (Fig.4.9) is sharper and shifted to the lower degree two theta when temperature is increased, because of the larger pore sizes. Fig 4.9b also shows the peak of 210 reflection which indicative of better quality of MCM-41 due to higher rate of diffusion of silicate anion at the higher temperature and the catalytic effect of higher surfactant ratio.

#### 4.5 Conclusions

Silatrane precursor synthesized by OOPS process is a very good alkoxide precursor to successfully synthesize very high surface area molecular sieve, MCM-41. While MCM-41 structure forms only in a narrow range of ion concentration, it can be synthesized in a wide range of temperature. The higher the temperature used, the larger the pore size. At the mixing temperature of 100°C, a high quality MCM-41 is observed. Surfactant concentration affected BET surface area while no effect on pore size was observed. The surface area of MCM-41 obtained at the surfactant ratio of 0.6 and 60°C is as high as 2400 m<sup>2</sup>/g. The pore volume obtained at the same surfactant ratio and 100°C is 1.72 cc/g. High surface area, precise structure and large pore volume make this material useful in catalysis area since higher surface area will allow higher catalyst concentration to be present. Moreover, precise structure will provide higher selectivity in applications involving size-based separation.

#### 4.6 Acknowledgements

This research work is supported by the Postgraduate Education and Research Program in Petroleum and Petrochemical Technology (ADB) Fund, Ratchadapisake Sompote Fund, Chulalongkorn University and the Thailand Research Fund (TRF).

#### 4.7 References

1. X. S. Zhao, G. Q. Lu, J.M. Graeme, *Ind. Eng. Chem. Res.* 1996, 35, 2075-2090.
2. J.B. Thomas, M.B. Lucy, G.K. Walter, A.L. Douglas, M. Brain, A.M. Peter, P. Guido, W.S. George, C.V. Jame, M.Y. Omar, *Chem. Mater.* 1999, 11, 2633-2656.
3. S. Bernd, P. Sebastian, A. Markus, *J. Phys. Chem. B* 2001, 105, 10473-10483.
4. Y. Jackie, P.M. Christian, S.W. Michael, *Angew. Chem. Int. Ed.* 1999, 38, 56-77.
5. J.E. Haskouri, S. Cabrera, M. Caldes, J. Alamo, A. Beltran-Porter, M.D. Marcos, P. Amoros, D. Beltran-Porter, *Int. J. Inorg. Mater.* 2001, 3, 1157-1163.
6. J.E. Haskouri, S. Cabrera, M. Caldes, J. Alamo, A. Beltran-Porter, M.D. Marcos, P. Amoros, D. Beltran-Porter, *Chem. Mater.* 2002, 14, 2637-2643.
7. S. Cabrera, J.E. Haskouri, G. Carmen, L. Julio, A. Beltran-Porter, D. Beltran-Porter, M.D. Marcos, P. Amoros, *Solid State Science* 2000, 2, 405-420.
8. J.G. Verkade, *Acc. Chem. Res.* 1993, 26, 483-489.
9. J. Pinkas, J. Verkade, *Inorg. Chem.* 1993, 32, 2711-2721.
10. W. Charoenpinijkarn, M. Sawankruhasn, B. Kesapabutr, S. Wongkasemjit, A.M. Jamieson, *Eur. Polym. J.* 2001, 37, 1441-1448.
11. S. Thitinum, N. Thanabodeekij, A.M. Jamieson, S. Wongkasemjit, *J. Eur. Cer. Soc.* 2003, 23, 417-427.
12. M. Sathupanya, E. Gulari, S. Wongkasemjit, *J. Eur. Cer. Soc.* 2002, 22, 1293-1303.
13. M. Sathupanya, E. Gulari, S. Wongkasemjit, *J. Eur. Cer. Soc.* 2003, 23, 2305-2314.
14. P. Phiriyawirut, R. Magaraphan, A.M. Jamieson, S. Wongkasemjit, *Mat. Sci. Eng.* 2003, A361, 147-154.
15. J.S. Beck, J.C. Vartuli, W.J. Roth, M.E. Leonowicz, C.T. Kresge, K.D. Schmitt, C. Chu, D.H. Olson, E.W. Sheppard, S.B. McCullen, J.B. Higgins, J.L. Schlenker, *J. Am. Chem. Soc.* 1992, 114, 10834-10843.
16. S. Schacht, M. Janicke, F. Schuth, *Microporous Mesoporous Mater.* 1998, 22, 485-493.

17. Z. Liu, Y. Sakamoto, T. Ohsuna, K. Hiraga, O. Terasaki, C.H. Ko, H.J. Shin, R. Ryoo, *Angew. Chem. Int. Ed.* 2000, 39, 3107-3110.
18. J.H. Client, *Surfactant Aggregation*, Blackie& Son Ltd: London, 1992.
19. W. Zhou, J. Klinowski, *Chem. Phys. Lett.* 1998, 292, 207-211.
20. F.C. Cheng, W. Zhou, J. Klinowski, *Chem. Phys. Lett.* 1996, 263, 247-252.
21. M. Kruk, M. Jaroniec, A. Sayari, *J. Phys. Chem. B.* 1999, 103, 4590-4598.
22. D. Khushalani, A. Kuperman, G.A. Ozin, K. Tanaka, J. Garces, M.M. Olken, N. Coombs, *Adv. Mater.* 1995, 7, 842-248.
23. T.P. Tanev, T.J. Pinnavaia, *Chem. Mater.* 1996, 8, 2068-2979.
24. Q. Huo, D.I. Magolese, G.D. Stucky, *Chem. Mater.* 1996, 8, 1147-1160.
25. P. Feng, X. Bu, D.J. Pine, *Langmuir*, 2000, 16, 5304-5310.
26. A. Sayari, S. Hamoudi, *Chem. Mater.* 2001, 13, 3151-3168.
27. J.I. Kroschwitz, *Encyclopedia of Chemical Technology*, John Willey& Sons: USA, 1997.
28. G. Ertl, H. Knozinger, J. Weitkamp, *Handbook of Heterogeneous Catalysis*, VCH: Weinheim, 1997.
29. D.H. Park, C.F. Cheng, J. Klinowski, *Bull. Korean. Chem. Soc.*, 1997, 18, 379-384.
30. C.F. Cheng, Z. Luan, J. Klinowski, *Langmuir* 1995, 11, 2815-2819.

**Table 4.1** The BET analysis of MCM-41 synthesized at different NaOH ratio 0.25 and 0.35

NaOH ratio	BET Surface Area (m <sup>2</sup> /g)	Pore volume (cc/g)	Average Pore size (Å)
0.25	1850	1.015	22
0.35	1100	0.711	25

**Table 4.2** The BET analysis of MCM-41 synthesized at different temperatures

Temperature (°C)	BET Surface Area (m <sup>2</sup> /g)	Pore Volume (cc/g)	Average Pore Size (Å)
40	2050	1.060	21
60	2098	1.188	22
80	1630	1.333	33
100	1550	1.080	35

**Table 4.3** The BET analysis of MCM-41 synthesized at different aging times

Aging Time (hr)	BET Surface Area (m <sup>2</sup> /g)	Pore Volume (cc/g)	Average Pore Size (Å)
1	1812	1.101	24
2	2054	1.188	22
3	2098	1.015	22
6	2044	1.165	23
12	2085	1.153	22

**Table 4.4** The BET analysis of MCM-41 synthesized at different surfactant ratios and temperatures

Surfactant ratio	BET Surface Area (m <sup>2</sup> /g)	Pore Volume (cc/g)	Average Pore Size (Å)
<b><u>60°C</u></b>			
0.2	1952	1.047	21
0.3	2098	1.188	22
0.4	2278	1.311	23
0.6	2430	1.288	22
<b><u>100°C</u></b>			
0.3	1550	1.080	35
0.4	1900	1.560	34
0.6	2100	1.723	33

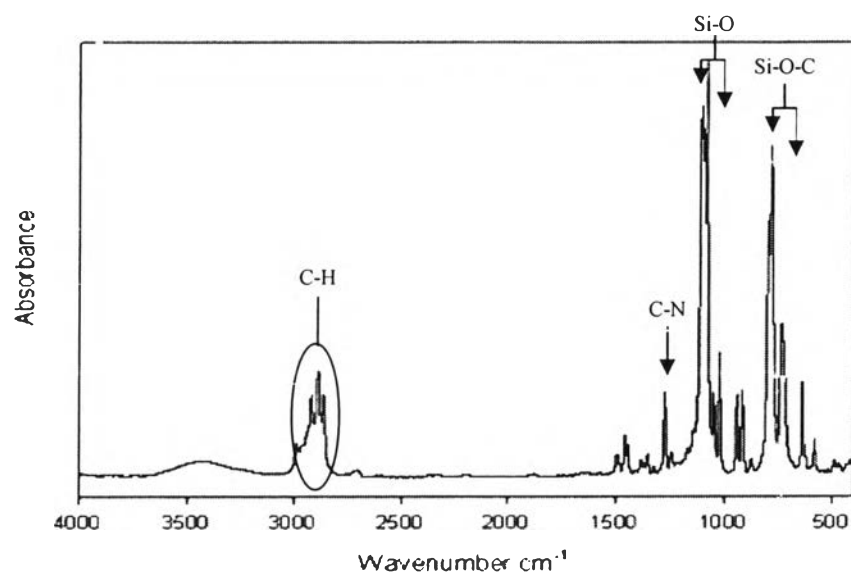


**Figure 4.1** FT-IR spectrum of synthesized silatrane precursor.



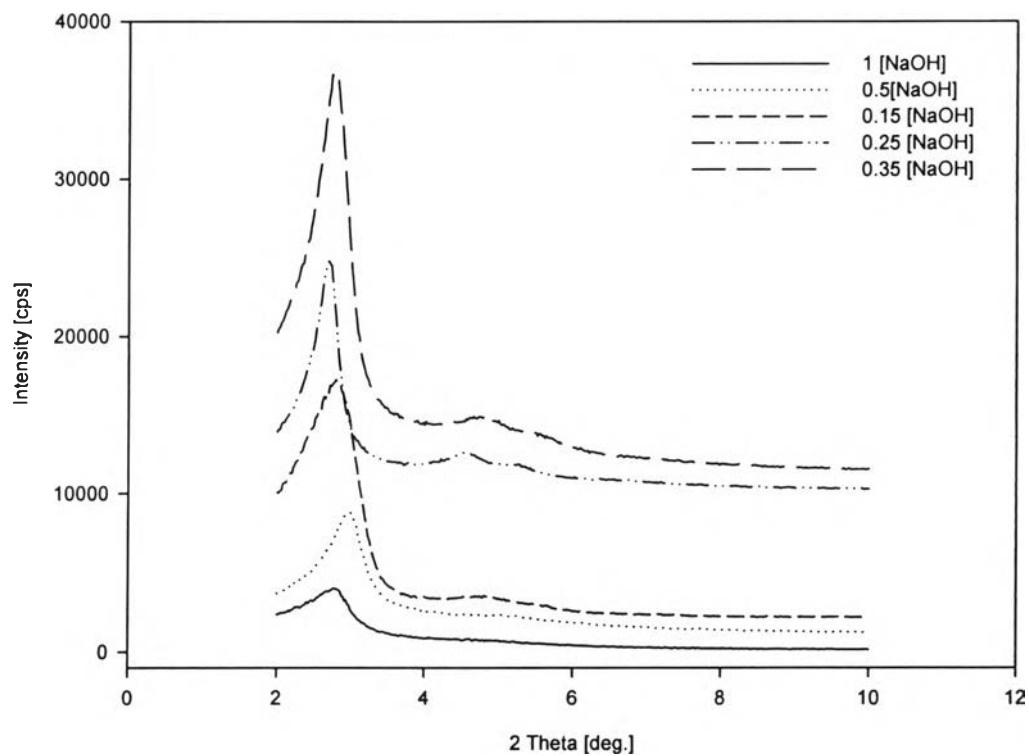


**Figure 4.2** XRD spectra of synthesized MCM-41 as a function of ion concentration.

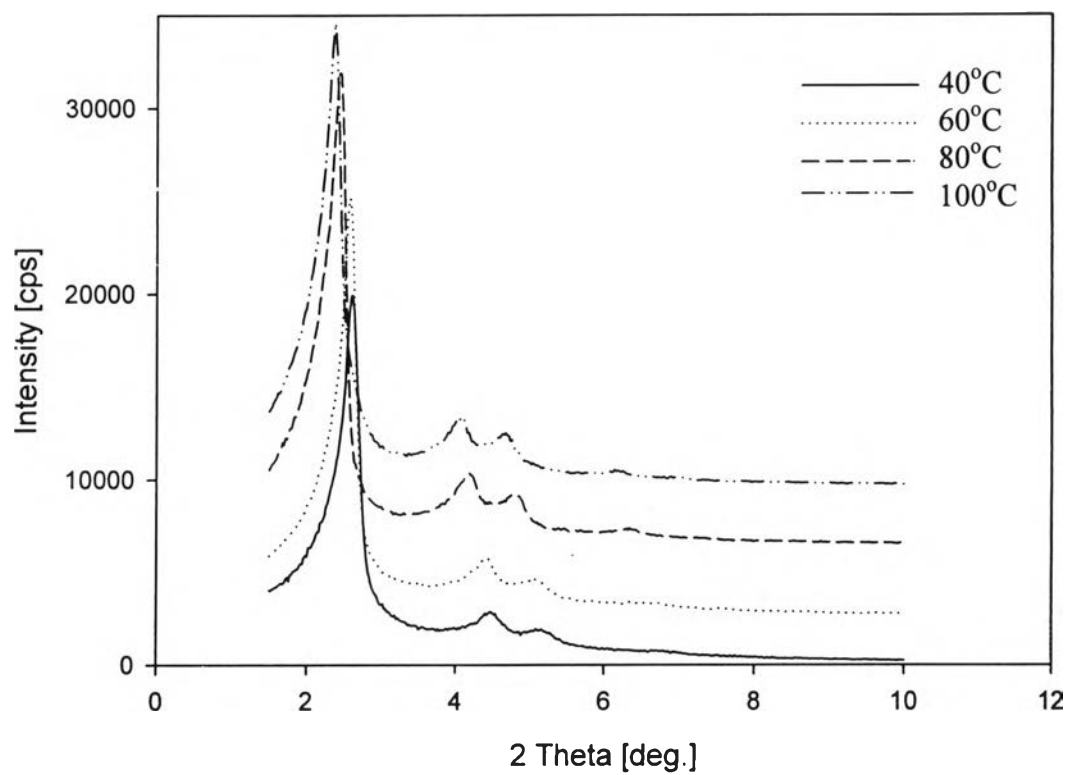


**Figure 4.3** XRD spectra of synthesized MCM-41 as a function of synthesis temperature.

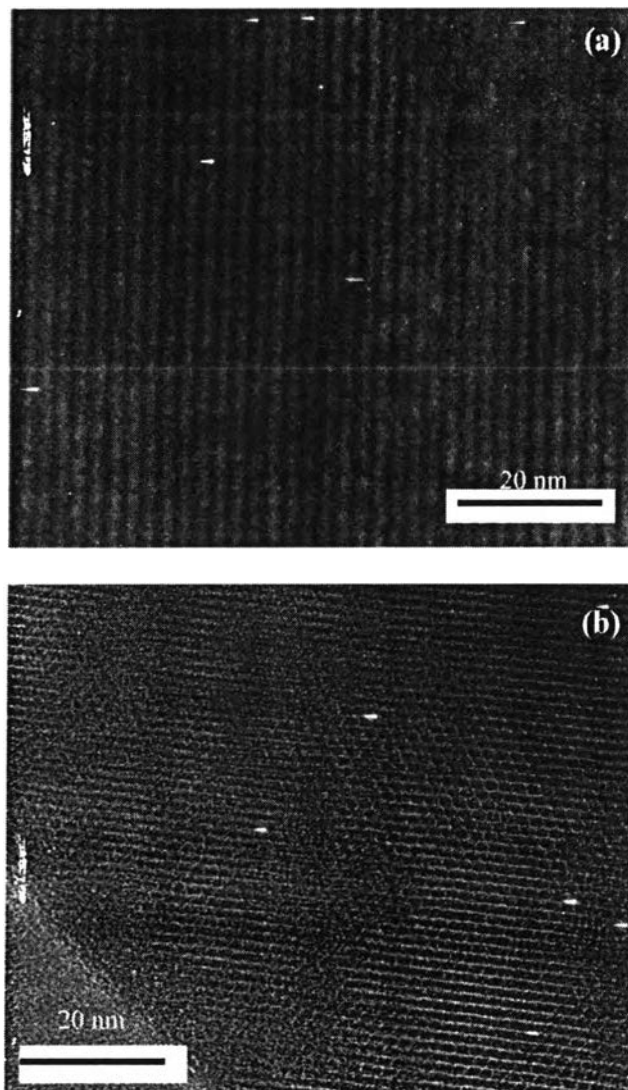


**Figure 4.4** TEM images of hexagonal arrangement, MCM-41, at 60°C: (a) along the channel and (b) perpendicular the channel.

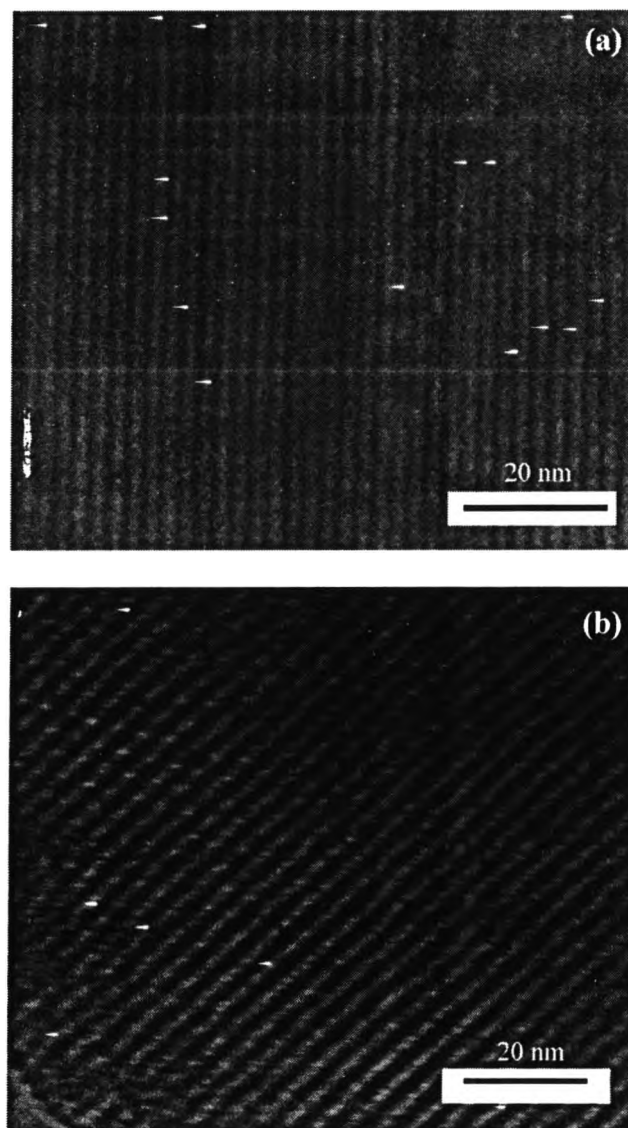


**Figure 4.5** Effect of temperature on TEM image of MCM-41 at: (a) 60°C and (b) 100°C.

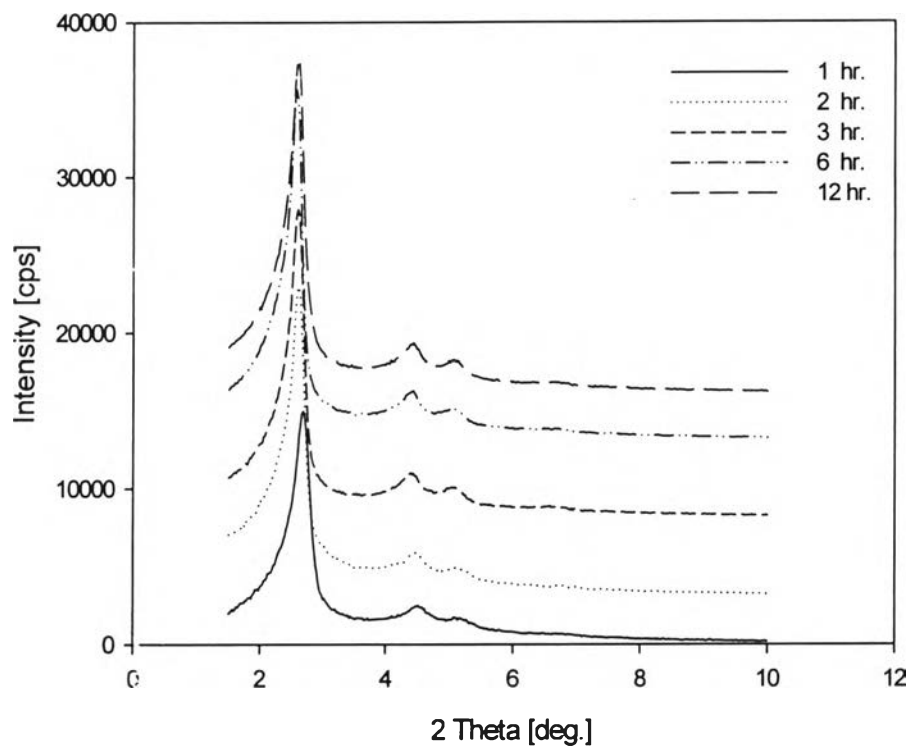


**Figure 4.6** Effect of aging time on XRD spectra of MCM-41 synthesized at 60°C.

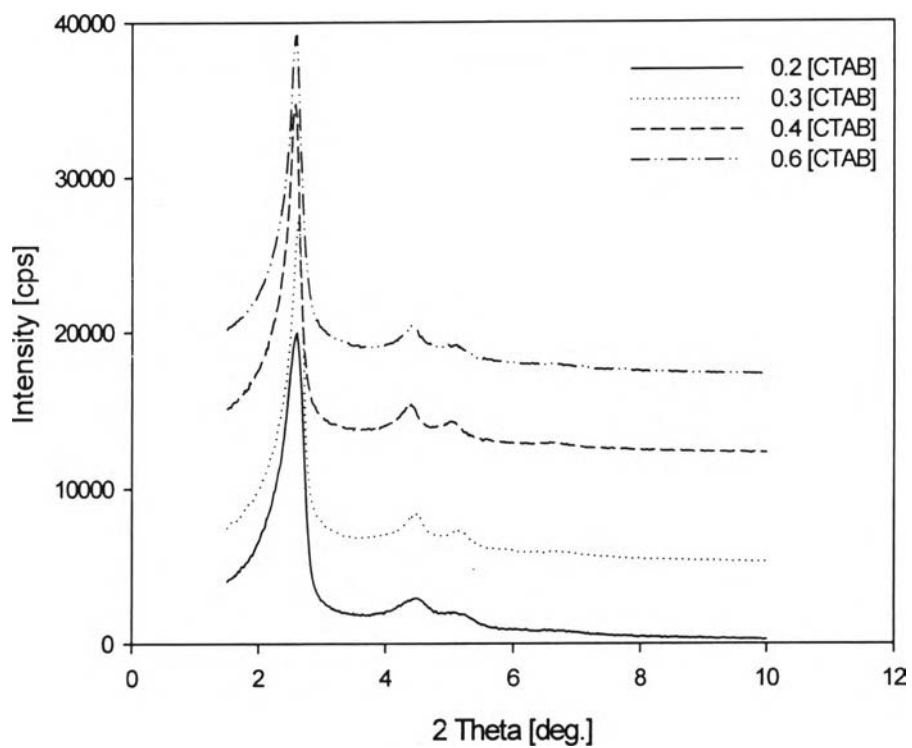


**Figure 4.7** Effect of surfactant concentration on XRD spectra of MCM-41 synthesized at 60°C.

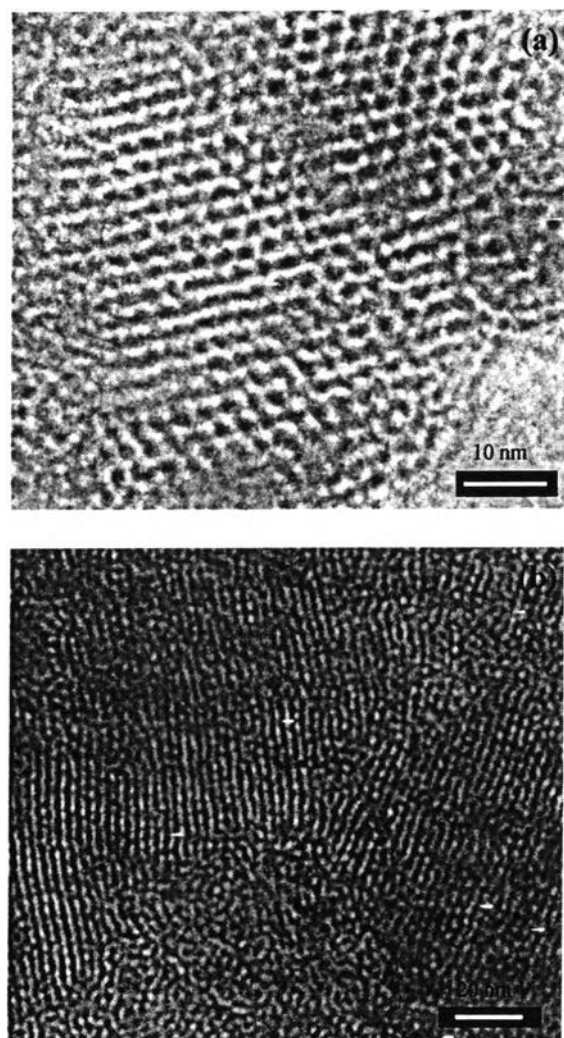


**Figure 4.8** TEM images of hexagonal MCM-41 arrangement at the surfactant ratio of 0.6.

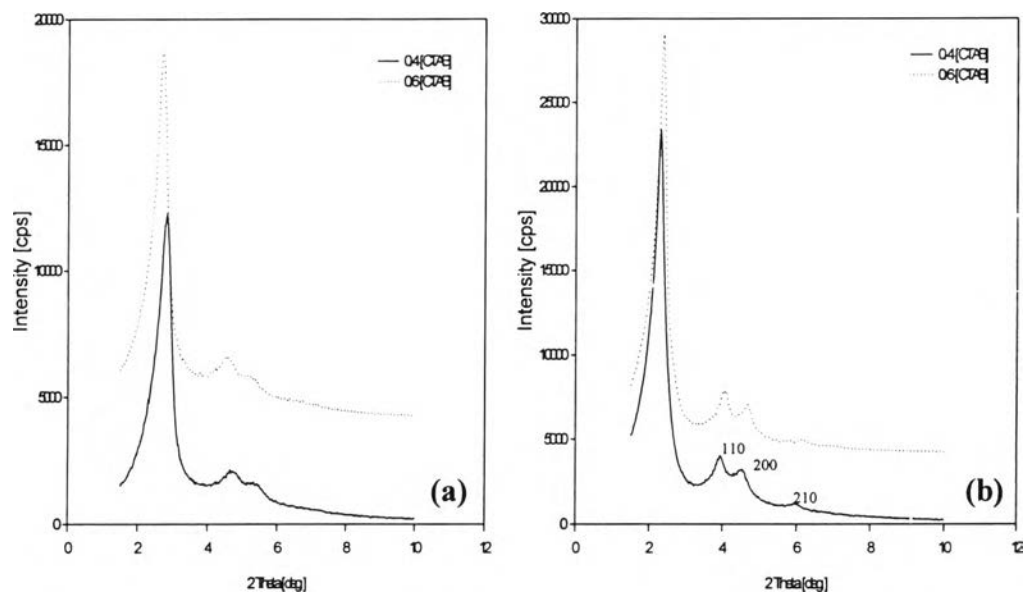


**Figure 4.9** Effect of temperature on XRD spectra of MCM-41 at the surfactant ratio of 0.6 and the mixing temperature of: **(a)** 60° and **(b)** 100°C.